



# Taohong Siwu Decoction exerts anticancer effects on breast cancer via regulating *MYC*, *BIRC5*, *EGF* and *PIK3R1* revealed by HTS<sup>2</sup> technology



Yu Gui<sup>a</sup>, Yifei Dai<sup>c</sup>, Yumei Wang<sup>b</sup>, Shengrong Li<sup>a</sup>, Lei Xiang<sup>b</sup>, Yuqin Tang<sup>b</sup>, Xue Tan<sup>b</sup>, Tianli Pei<sup>b</sup>, Xilinqiqige Bao<sup>d,\*</sup>, Dong Wang<sup>a,b,\*</sup>

<sup>a</sup> State Key Laboratory of Southwestern Chinese Medicine Resources, School of Pharmacy, School of Basic Medical Sciences, Chengdu University of Traditional Chinese Medicine, Chengdu 611137, China

<sup>b</sup> School of Basic Medical Sciences, Chengdu University of Traditional Chinese Medicine, Chengdu 611137, China

<sup>c</sup> Department of Basic Medical Sciences, School of Medicine, Tsinghua University, Beijing 100084, China

<sup>d</sup> Medical Innovation Center for Nationalities, Inner Mongolia Medical University, Hohhot City 010110, China

## ARTICLE INFO

### Article history:

Received 21 February 2022

Received in revised form 20 June 2022

Accepted 21 June 2022

Available online 26 June 2022

### Keywords:

Taohong Siwu Decoction

Breast cancer

HTS<sup>2</sup> technology

Bioinformatics

Systems pharmacology

## ABSTRACT

Taohong Siwu Decoction (TSD), a classical gynecological prescription that was firstly reported 600 years ago, has been widely used in the adjuvant treatment of breast cancer (BRCA) in China. However, the mechanism of action of TSD in treating BRCA has remained unclear. Here, high-throughput sequencing-based high-throughput screening (HTS<sup>2</sup>) technology was used to reveal the molecular mechanism of TSD, combination with bioinformatics and systems pharmacology in this study. Firstly, our results showed that TSD exerts an anticancer effect on BRCA cells by inhibiting cell proliferation, migration and inducing apoptosis as well as cell-cycle arrest. And our results from HTS<sup>2</sup> suggested that herbs of TSD could significantly inhibit KRAS pathway and pathway in cancer, and activate apoptosis pathway, p53 pathway and hypoxia pathway, which may lead to the anticancer function of TSD. Further, we found that TSD clearly regulates *MYC*, *BIRC5*, *EGF*, and *PIK3R1* genes, which play an important role in the development and progression of tumor and have significant correlation with overall survival in BRCA patients. By molecular docking, we discovered that Pentagalloylglucose, a compound derived from TSD, might directly bind to and inhibit the function of BRD4, which is a reported transcriptional activator of *MYC* gene, and thus repress the expression of *MYC*. Taken together, this study explores the mechanism of TSD in anti-BRCA by combining HTS<sup>2</sup> technology, bioinformatics analysis and systems pharmacology.

© 2022 The Author(s). Published by Elsevier B.V. on behalf of Research Network of Computational and Structural Biotechnology. This is an open access article under the CC BY-NC-ND license (<http://creativecommons.org/licenses/by-nc-nd/4.0/>).

## 1. Introduction

Breast cancer (BRCA) is the most frequently diagnosed malignancy among women worldwide. Published epidemiological reports show a significant increase in the mortality rate of BRCA in the past two decades [1]. Despite great advances in the early detection of BRCA and the development of effective therapies, it continues to be the second leading cause of cancer-associated mortality among all malignancies [2]. According to the different subtypes of BRCA, various therapeutic strategies can be used to eliminate tumor cells, such as chemotherapy, radiotherapy, surgery, and hormone therapy [3]. However, these conventional ther-

apies also have disadvantages such as side effects and drug resistance. Therefore, as an important form of complementary and alternative medicine, traditional Chinese medicine (TCM) has emerged into clinically adjuvant treatments of BRCA in recent years because of its relatively few side effects and low costs [4].

Taohong Siwu Decoction (TSD), a prescription for BRCA clinically adjuvant treatment, originates from a historic medical book named *Yizong Jinjian* (Qing Dynasty, 1742 CE). TSD is composed of six herbs, including *Persicac Semen* (Taoren), *Carthami Flos* (Honghua), *Rehmanniae Radix Praeparata* (Shudihuang), *Angelicae Sinensis Radix* (Danggui), *Paeoniae Radix Alba* (Baishao), and *Chuanxiong Rhizoma* (Chuanxiong). It has been reported that TSD can interfere with BRCA *in vivo* [5–7]. While there is still few research on mechanism of action of TSD in the treatment of BRCA.

High-throughput sequencing-based high-throughput screening (HTS<sup>2</sup>), combining RNA annealing, selection, ligation (RASL) strategy with next-generation sequencing technology, enables the

\* Corresponding authors at: State Key Laboratory of Southwestern Chinese Medicine Resources, School of Pharmacy, School of Basic Medical Sciences, Chengdu University of Traditional Chinese Medicine, Chengdu 611137, China (D. Wang).

E-mail addresses: [2528325529@qq.com](mailto:2528325529@qq.com) (X. Bao), [dwang@cduetcm.edu.cn](mailto:dwang@cduetcm.edu.cn) (D. Wang).

detection of the expression of thousands of genes in cells treated with hundreds of herbs [8]. It can be used to quantitatively analyze gene matrices related to a specific pathway to screen out potential drugs [9]. Moreover, it can be applied in large-scale herb treated cell gene studies that offer novel perspectives in research into TCM [10–11]. In comparison with conventional screening strategies, HTS<sup>2</sup> has several advantages, namely, cost-effectiveness, time-savings, and higher reproducibility [12].

Bioinformatics is the application of tools of computation and analysis to the capture and interpretation of biological data, which is useful in studying genomes and DNA sequencing [13]. Recent years, systems pharmacology, as an emerging interdisciplinary approach, has been widely used to reveal complex mechanisms of TCM formulae by using bioinformatics and identify potential active compounds present in them [14].

Therefore, in the present study, we evaluate the potential anti-cancer effects of TSD on BRCA cells and explore the underlying mechanisms based on HTS<sup>2</sup> technology and bioinformatics. Firstly, the effects of TSD on proliferation, apoptosis, cell cycle and migration were assessed in BRCA cells. Then, systems pharmacology was utilized to identify potential active compounds present in TSD and explore the underlying mechanism. Moreover, HTS<sup>2</sup> was used to detect the effect of herb intervention on gene expression. Further bioinformatics was performed to identify hub genes and to explain its anti-BRCA mechanism. Finally, molecular docking was conducted to explore the potential inhibitors in TSD.

## 2. Materials and methods

### 2.1. Preparation of TSD and HPLC analysis

The six herbs of TSD were purchased from Beijing Tong-Ren-Tang (Chengdu, China). In accordance with the clinic dose, each herb was weighed precisely and then the herbs were mixed and immersed in 90% ethanol overnight (Table S1). Subsequently, the mixture was extracted three times (for 1 h each time) with a heating mantle. Next, the ethanolic extracts were merged, evaporated to dryness under reduced pressure and then preserved in a refrigerator at –80 °C. Furthermore, TSD was assayed by a Thermo Scientific UltiMate 3000 HPLC system equipped with a diode array detector. A reverse phase Agilent C18 column (250 mm × 4.6 mm, 5 μm) was used and kept at 30 °C. The mobile phase consisting of aqueous phosphoric acid solution and acetonitrile was used with a gradient elution at a flow rate of 1.0 ml/min (Table S2). The UV spectrophotometer detector was set at 280 nm.

### 2.2. Cell culture and cell viability assay

Human triple-negative breast cancer cell lines (MDA-MB-231) were purchased from the National Infrastructure of Cell Line Resource (Beijing, China) and cultured in Dulbecco's Modified Eagle Medium (DMEM, Gibco, ThermoFisher, China) containing 10% fetal bovine serum (FBS, Gemini, USA), 100U/ml streptomycin and penicillin (HyClone™, Utah, USA) under a humidified atmosphere of 5% CO<sub>2</sub> at 37 °C. Then, to assess cell viability, symmetrically separate MDA-MB-231 cells were piped into a 96-well plate at a density of  $7 \times 10^3$  cells per well. After overnight incubation, the cells were mixed with TSD at concentrations that ranged from 125 μg/ml to 6 mg/ml for 48 h. Then, 10 μl prepared CCK-8 reagent was added to each well to produce a chromogenic reaction. The optical density, which indicating the cell viability, was measured at 450 nm.

### 2.3. Flow cytometry staining and analysis assay

In order to determine the effect of TSD on cell apoptosis, the MDA-MB-231 cells were seeded onto 6-well plate ( $2 \times 10^5$  cells per well). After overnight incubation, the cells were treated with different concentrations (0.5 mg/ml, 1 mg/ml, and 2 mg/ml) of TSD for 24 h. The cells were resuspended in 195 μl binding buffer, then were stained with 5 μl FITC-Annexin-V and 10 μl propidium iodide (Beyotime, China) in the dark for 15 min. The apoptosis rates of the cells were analyzed using flow cytometry (BD, Biosciences, USA).

To determine cell cycle activity, the MDA-MB-231 cells were treated with different concentrations (0.5 mg/ml, 1 mg/ml, and 2 mg/ml) of TSD for 24 h, and then were fixed with 70% ethanol overnight at –20°C. After that, cells were washed with PBS and resuspended in 500 μl PI/RNase Staining Buffer (BD, USA) in the dark at 4°C for 15 min. The cell cycle analysis was conducted using flow cytometry.

### 2.4. Wound healing assay

To determine wound healing, the MDA-MB-231 cells were seeded onto 96-well plate ( $1 \times 10^4$  cells per well). After overnight incubation, the wound line was made by auto-scratch wound making tool and the cell debris was washed several times with PBS, and the cells were cultured with FBS-free medium containing different concentrations (0.5 mg/ml, 1 mg/ml, and 2 mg/ml) of TSD for 24 h. Images of wound healing were captured through Incucyte® SX1 Live-Cell Analysis System.

### 2.5. Collection of chemical constituents, therapeutic targets and prediction of putative targets

All the chemical constituents of the six herbs present in TSD were retrieved from the Traditional Chinese Medicine Systems Pharmacology Database (TCMSP) (<http://tcmsp.com/tcmsp.php>) [15], the Chemistry Database (CSDb) ([www.orgchem.csdb.cn/scdb/default.asp](http://www.orgchem.csdb.cn/scdb/default.asp)), and the Traditional Chinese Medicines Integrated Database (TCMID) (<http://119.3.41.228:8000/tcmid/>) [16]. Subsequently, all the targets associated with the chemical compounds present in TSD were predicted using SwissTargetPrediction (<https://www.swisstargetprediction.ch/>) [17]. To ensure the reliability of the results of target prediction, targets with a probability score of > 0 were regarded as potential targets of compounds. Then, BRCA-related targets were selected from three web resources, of which one was Online Mendelian Inheritance in Man (OMIM) (<https://omim.org/>, updated on Jun 28, 2019) [18]. Another resource used was DrugBank (<https://www.drugbank.ca/>, updated Jul 2, 2019) [19]. The third resource used was the Therapeutic Target Database (TTD) (<http://db.idrblab.net/ttd/>, updated Sep 15, 2017) [20].

### 2.6. HTS<sup>2</sup> assay

HTS<sup>2</sup>, as a high-throughput screening technique, provides an opportunity to produce large-scale cell transcriptional data in the context of herbal perturbations. The HTS<sup>2</sup> assay mainly comprised cell culture, treatment with herb extracts, probe design, and screening. In this research, HTS<sup>2</sup> assay was carried out to detect the regulation of six herbal extracts in TSD on a total of 2336 genes in MDA-MB-231 cells, which was in accordance with our previous report [10–11].

## 2.7. HTS<sup>2</sup> data processing

Initially, all reads were mapped to the probe sequences and normalized with respect to the expression of stable housekeeping genes. Afterward, R software was utilized to calculate Pearson correlation coefficients among normalized transcriptional data following treatments with 16 replicates of dimethyl sulfoxide (DMSO) and three replicates of the six herbs present in TSD, in order to assess reliability and repeatability of the transcriptional data. Correlation coefficients > 0.9 suggested that the results of the HTS<sup>2</sup> assay were reliable and repeatable. Subsequently, the R package DESeq2 [21] was employed to calculate the foldchange (FC) and *P*-value of gene expression, and gene expression changes with |FC| > 2 and a *P*-value of < 0.05 were regarded as differentially expressed genes (DEGs). Finally, the heatmap and volcano plots of DEGs were plotted using the R package pheatmap and ggplot2, respectively [22].

## 2.8. Gene set enrichment analysis

GSEA was adopted to evaluate the effect of each herb in TSD on different gene set. In this method, ranked differentially expressed genes list of each herb and gene set were used. Genes were aligned to the ranked list, followed by calculation of the running sum [23]. As a result, the enrichment scores were obtained and normalized to obtain the Normalized enrichment score (NES). Meanwhile, the false discovery rate (FDR) was calculated, and an FDR < 0.25 indicated statistical significance.

## 2.9. Protein-protein interaction network and functional enrichment analysis

In order to identify the hub genes, total DEGs after removing duplicates from each herb were used to construct the PPI network via STRING database [24], followed by the topological analysis by Cytoscape software [25]. Meanwhile, functional enrichment analysis was performed to examine the biological functions of these DEGs, including Gene Ontology (GO), and Kyoto Encyclopedia of Genes and Genomes (KEGG) via DAVID database [26]. The enrichment of GO terms and KEGG signaling pathways were remained based on the adjusted *P*-value of < 0.05, followed by visualization of the top 10 most significant GO terms and KEGG signaling pathways.

## 2.10. Gene expression level and survival analysis

Clinical information and transcriptomic data of 1195 BRCA samples were collected from The Cancer Genome Atlas (TCGA) data portal [27]. While there were too few *para*-cancerous samples in BRCA tumor, a total of 179 healthy tissues and organs from The Genotype-Tissue Expression Project (GTEx) database were collected [28]. To compare a gene's expression level between tumor and matched normal tissues, normalized counts distribution in tumors versus normal tissues were analyzed by Wilcoxon Test. Subsequently, each tumor sample was divided into high or low expression group according to gene expression value and then utilized the cox proportional hazard model for association evaluation between gene expression and patient overall survival in BRCA.

## 2.11. Real-Time quantitative PCR analysis

Total RNA from cultured cells was isolated by using TRIzol (Vazyme Biotech Co., Ltd, China), then reversely transcribed into cDNA using HiScript II Q RT SuperMix for qPCR kit (Vazyme, China). Gene expression was assessed by a real-time PCR reaction using the ChamQ Universal SYBR qPCR Master Mix (Vazyme, China). The relative level of gene expression was normalized to GAPDH.

The full list of primer pairs used in this study is provided in Table S3.

## 2.12. Molecular docking

The X-ray crystal structures of proteins with ligands were retrieved from the Protein Data Bank database [29]. Subsequently, each protein was prepared using "Protein Preparation Wizard" of Schrödinger software (Schrödinger Release, 2019–1). In addition, the LigPrep module was utilized to generate the 3D structures and minimize the energies of the selected compounds present in TSD. The receptor-grid generation module was used to form a grid box, and all molecular docking calculations were conducted by applying Glide XP docking. Finally, the ligand interaction diagram module was employed for the visualization of ligand-protein interactions.

## 2.13. Western blot analysis

MDA-MB-231 cells treated with DMSO and Pentagalloylglucose were lysed RIPA lysis buffer with complete protease inhibitor cocktail for 30 min at 4 °C, then centrifuged at 12,000 × *g* for 15 min at 4 °C. And the concentrations were determined by BCA protein assay kit. Cell extracts were boiled for 5 min at 100 °C, and the protein samples were subjected to electrophoresis on 10% SDS-polyacrylamide gels, then transferring to PVDF membranes. They were blocked with 5% BSA for 1 h and probed with specific primary antibodies with appropriate dilution at 4 °C overnight. The membranes were washed with TBST three times, each time for 10 min, and incubated with secondary antibodies for 1.5 h, followed by three washes. Lastly, the immune-reactive bands were observed by ECL kit.

## 2.14. Statistical analysis

Statistical analyses of experimental data were executed in triplicate via Student's *t*-test. All data are presented as mean values and standard errors. The levels of significance were set at \**P* < 0.05, \*\**P* < 0.01, \*\*\**P* < 0.001.

# 3. Results

## 3.1. HPLC analysis of TSD

The identification of TSD constituents was based on the retention time and the UV spectrum at a wavelength of 280 nm. Nine components in the six herbs were identified with the indicated conditions (Fig. S1).

## 3.2. Determination of effect of TSD on biological capabilities of MDA-MB-231 cells

MDA-MB-231 cells were treated with different-concentration TSD and vehicle, then cell viability was determined by a CCK-8 assay. The results showed that the IC<sub>50</sub> value was 1896 μg/ml (Fig. S2A), which indicated that a high-concentration TSD exerts an inhibitory effect on the proliferation of MDA-MB-231 cells. In order to determine whether TSD has an effect on promoting apoptosis of BRCA cells, flow cytometric analysis of MDA-MB-231 cells treated with different-concentration TSD and vehicle was employed. The results showed that a high-concentration TSD (2 mg/ml, 24 h) significantly promoted apoptosis (Fig. 1A, S2B), while a low- or mid-concentration TSD (0.5 mg/ml, 1 mg/ml, 24 h) had inconspicuous effect. To determine whether TSD has an effect on cell-cycle arrest, flow cytometry for DNA content in

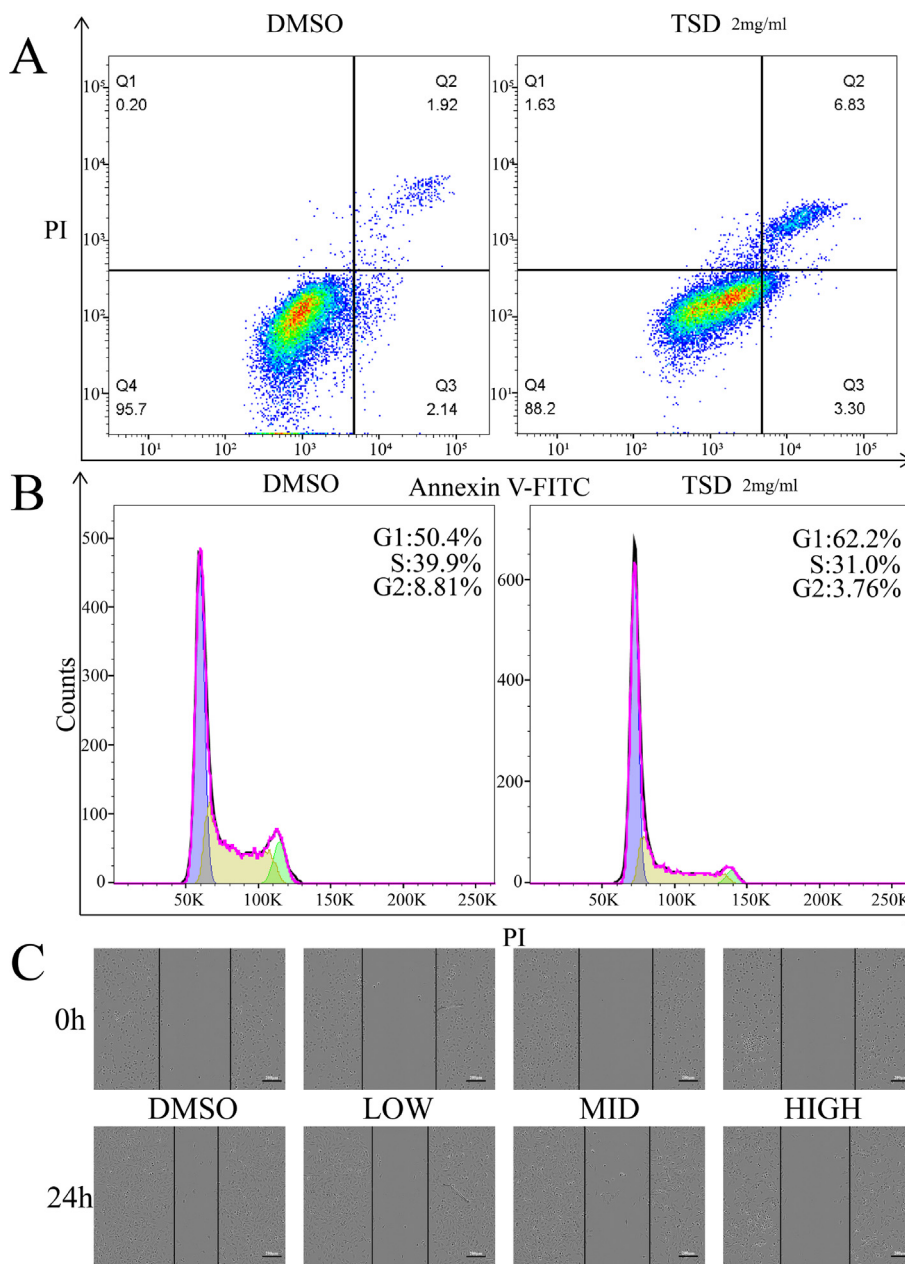


**Fig. 1.** Effect of TSD on biological capabilities of MDA-MB-231 cells. (A) Flow cytometric analysis of MDA-MB-231 cells treated with high-concentration TSD and vehicle. Apoptotic cells were determined by Annexin V and propidium iodide stains. (B) Flow cytometry for DNA content in MDA-MB-231 cells. High-concentration TSD (2 mg/ml, 24 h) induced a G1 arrest compared to DMSO. (C) Effect of TSD on the migration of MDA-MB-231 cells, determined by wound healing assay.

MDA-MB-231 cells was conducted. The results showed that a high-concentration TSD (2 mg/ml, 24 h) induced a G1 cell-cycle arrest compared to DMSO (Fig. 1B). Lastly, effect of TSD on the migration of MDA-MB-231 cells was determined by wound healing assay. The results showed that TSD significantly reduced the wound closure rate in MDA-MB-231 cells in a dose-dependent manner (Fig. 1C, S2C). In summary, TSD could inhibit proliferation, migration, and induce G1 phase arrest as well as apoptosis in MDA-MB-231 cells.

### 3.3. Construction of ingredient-target network and enrichment analysis

In order to explore the underlying mechanism of TSD in treating BRCA, systems pharmacology was initially utilized. Firstly, a total of 641 TSD-related active ingredients were retrieved from the

TCMSP, TCMID, and CSDB, including Shudihuang (35), Taoren (50), Baishao (58), Honghua (126), Chuanxiong (170) and Danggui (202) (Table S4). After that, all the active ingredients present in TSD were used to predict potential targets using SwissTargetPrediction, and targets with probability scores of >0 were selected (Table S5). Then, in order to identify all the BRCA-related therapeutic targets, a total of 182 known BRCA-related targets were retrieved from the TTD, OMIM, and DrugBank databases after the removal of duplicates (Table S6). Subsequently, to demonstrate the relationships between ingredients and targets, the ingredient-target network of TSD was constructed using Cytoscape. Specifically, this network is composed of 84 BRCA-related targets and 405 active ingredients (Fig. 2). Moreover, the PPI network of the 84 BRCA-related targets was constructed using STRING database and topological characteristics of this PPI network were calculated using the Network Analyzer plug-in (Fig. 3A). Further,

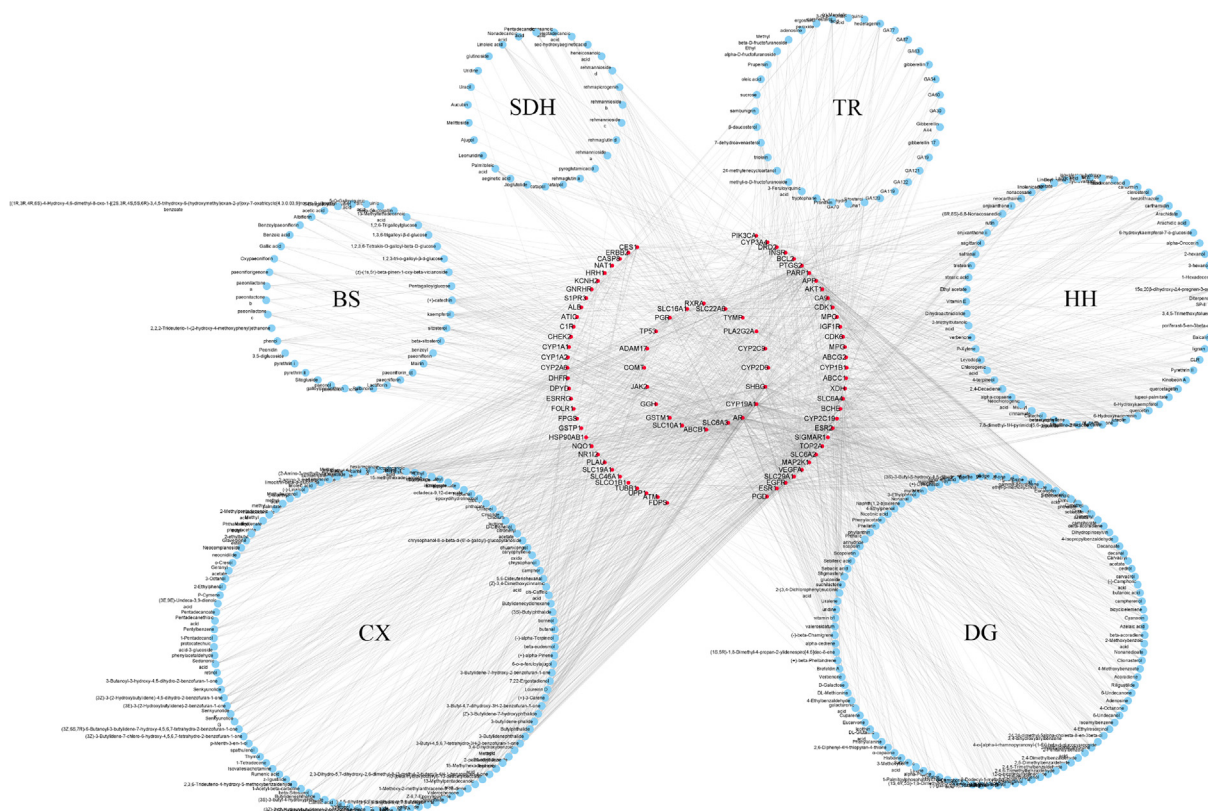


**Fig. 2.** The ingredient-target network of TSD. The red nodes represented BRCA targets and blue ones represented active ingredients. (TR, Taoren; HH, Honghua; BS, Baishao; CX, Chuanxiong; DG, Danggui; SDH, Shudihuang). (For interpretation of the references to color in this figure legend, the reader is referred to the web version of this article.)

KEGG/GO enrichment analysis was carried out to reveal the potential mechanisms associated with the 84 BRCA-related targets. The results of GO enrichment analysis indicated that these 84 BRCA-related targets were involved in multiple biological processes, significantly, including response to drug, oxidation-reduction process, and positive regulation of transcription from RNA polymerase II promoter (Fig. 3B). In addition, the results of KEGG enrichment analysis showed that the effect of TSD in treating BRCA is closely correlated with the KEGG terms “Metabolic pathways,” “Pathways in cancer,” and “PI3K-Akt signaling pathway” (Fig. 3C).

**3.4. Identification of DEGs and gene expression profiles treated with six herbs in MDA-MB-231 cells by HTS<sup>2</sup> assay**

MDA-MB-231 cells were treated with each herb in TSD and vehicle, then HTS<sup>2</sup> assay was employed to detect the expression changes in 2336 genes which involved in serious diseases such as cancer. As a result, the greatest number of DEGs were found in the cells with and without Honghua treatment, including 34 up-regulated and 19 down-regulated ones. While the fewest number of DEGs were identified in Taoren, a total of 16 DEGs, including 7 up-regulated and 9 down-regulated ones. Besides, 49, 40, 26 and 17 DEGs were identified in Chuanxiong, Baishao, Danggui and Shudihuang respectively (Fig. 4A). In order to investigate the relevancy of each herb, cluster analysis was employed to six herbs base on their similarities or differences of gene expression profile (Table S7). The results showed that six herbs of TSD were divided into three main categories: Honghua and Chuanxiong in group one, Baishao and Danggui in group two, Shudihuang and Taoren in group three (Fig. 4B).

**3.5. Investigation of effect of each herb in TSD on gene set analyzed by GSEA**

For further study on effect of each herb in TSD, GSEA was utilized to evaluate the overall effects of each herb on different gene set (Fig. S3, Table 1). As a result, Baishao had a significant negative regulation of “KRAS signaling up” which is related to promoting proliferation. In addition, Taoren and Danggui played an important role in negative regulation of “Pathway in cancer” that is related to promoting proliferation, migration as well as cell cycle and evading apoptosis. Moreover, Honghua possessed a positive regulation of “p53 pathway” and “apoptosis” which are related to apoptosis. Besides, Shudihuang had a negative regulation of “hypoxia” while Honghua and Chuanxiong had a positive regulation of it (Fig. 4C).

**3.6. Construction of PPI network and enrichment analysis**

After removing duplicates, a total of 168 DEGs were used to construct PPI network. Then, the topological characteristics of the PPI network were computed to investigate the hub genes whose degree centrality are twice more than average degree centrality among the whole network. As a result, MYC, PIK3R1, FOS, IL6, EGF, HIF1A, BCL2L1, SHC1, RPTOR, HMOX1, BIRC5, BCL6 and LIF were identified as hub genes (Fig. 5A, Table S8, S9). In order to explore the biological mechanisms among these 168 DEGs in TSD, the GO and KEGG enrichment analysis was conducted. The results of KEGG enrichment analysis showed that “pathways in cancer”, “cytokine-cytokine receptor interaction”, “Transcriptional misregulation in cancer” and “TNF signaling pathway” were the significant relevant signaling pathways (Fig. 5B). In addition, the results of GO enrichment analysis indicated that these 168 DEGs were involved

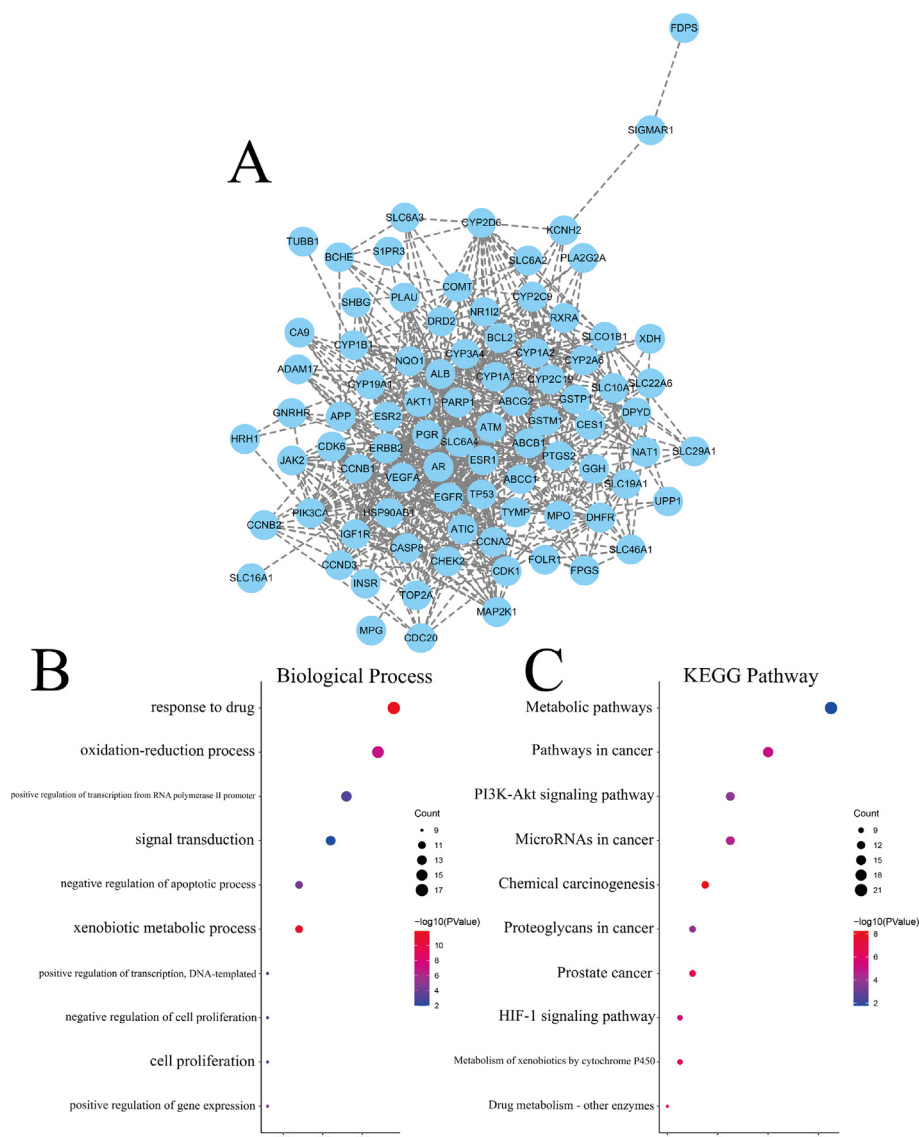


**Fig. 3.** Functional enrichment analysis of BRCA-related targets and PPI network analysis. (A) The PPI network of 84 BRCA-related targets. (B) GO enrichment analysis on 84 BRCA-related targets. (C) KEGG enrichment analysis on 84 BRCA-related targets.

in multiple biological processes, significantly, including positive regulation of transcription from RNA polymerase II promoter, negative regulation of apoptotic process, negative regulation of cell proliferation and positive regulation of apoptotic process (Fig. 5C).

### 3.7. Transcriptional level and prognostic value of hub genes in BRCA patients

To determine whether hub genes play an important role in clinical BRCA patients, transcriptional data from BRCA in the TCGA and GTEx databases were collected. Then transcriptional level of hub genes in BRCA was determined by joint analysis of BRCA data in TCGA matched with normal samples in GTEx. As a result, except for *HIF1A*, the rest of genes were highly significant differences between tumor tissues and adjacent tissues (Fig. 6A), which indicated that these genes play a critical role in BRCA development. Further investigating the effect of hub genes expression level on the prognosis of BRCA patients, the prognosis of each tumor sample in the TCGA was analyzed. The results showed that five genes had obvious correlation with overall survival of BRCA patients. High expression of *MYC*, *EGF*, *SHC1* and *PIK3R1* were correlated

with poor prognosis in BRCA patients, while low expression of *BIRC5* was positively correlated with poor overall survival (Fig. 6B). In summary, five hub genes, *MYC*, *BIRC5*, *EGF*, *SHC1* and *PIK3R1*, play an important role in the development and progression of tumor and have significant correlation with overall survival in BRCA patients.

### 3.8. Determination of effect of TSD on above five hub genes expression

In order to determine whether TSD has an effect on regulating above five hub genes expression, quantitative PCR was performed for *MYC*, *EGF*, *SHC1*, *BIRC5* and *PIK3R1*. As a result, TSD potently decreased expression of *MYC* gene which is a critical oncogene, *BIRC5* was also significantly downregulated in MDA-MB-231 cells treated with mid- and high-concentration TSD (1 mg/ml, 2 mg/ml, 24 h). While, TSD potently increased expression of *EGF* and *PIK3R1* gene which is a tumor suppressor gene (Fig. 6C). Whereas, *SHC1* was non-significantly regulated in MDA-MB-231 cells treated with TSD. In summary, four-fifths of hub genes were regulated by TSD, indicating that TSD exerts effects on proliferation, migration,

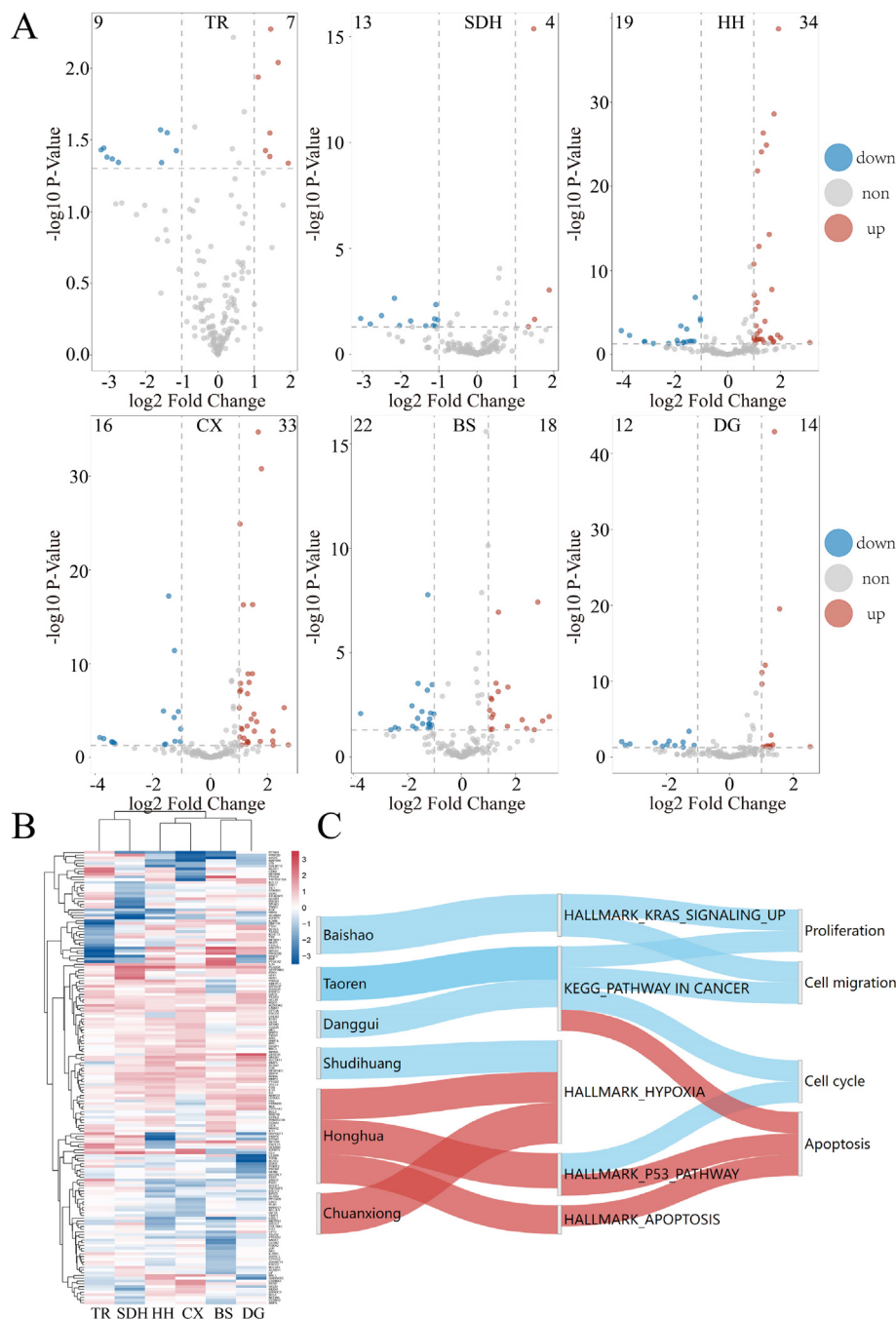


**Fig. 4.** DEGs of six herbs and gene expression profiles identified by HTS<sup>2</sup> assay and related gene set analyzed by GSEA. (A) The volcano plot of DEGs. The red spots represented up-regulated DEGs, while blue spots stood for down-regulated ones. (B) The heatmap of DEGs. The cluster analysis was employed to group six herbs into categories based on their similarities or differences of gene expression profile. (C) The Sankey Network associated with herb, gene set and biological capability. The bar color in blue stands for negative regulation, while red stands for positive regulation. (For interpretation of the references to color in this figure legend, the reader is referred to the web version of this article.)

**Table 1**  
Effect of six herbs based on Gene Set Enrichment Analysis.

| Gene Set                   | Herb       | Size | NES   | FDR   |
|----------------------------|------------|------|-------|-------|
| HALLMARK_KRAS_SIGNALING_UP | Baishao    | 10   | -1.77 | 0.004 |
| HALLMARK_APOPTOSIS         | Honghua    | 12   | 1.36  | 0.219 |
| HALLMARK_P53_PATHWAY       | Honghua    | 11   | 1.66  | 0.107 |
| HALLMARK_HYPOXIA           | Shudihuang | 17   | -1.49 | 0.143 |
| HALLMARK_HYPOXIA           | Chuanxiong | 17   | 1.94  | 0     |
| HALLMARK_HYPOXIA           | Honghua    | 17   | 1.45  | 0.19  |
| KEGG_PATHWAY IN CANCER     | Taoren     | 18   | -1.59 | 0.012 |
| KEGG_PATHWAY IN CANCER     | Danggui    | 17   | -1.3  | 0.159 |

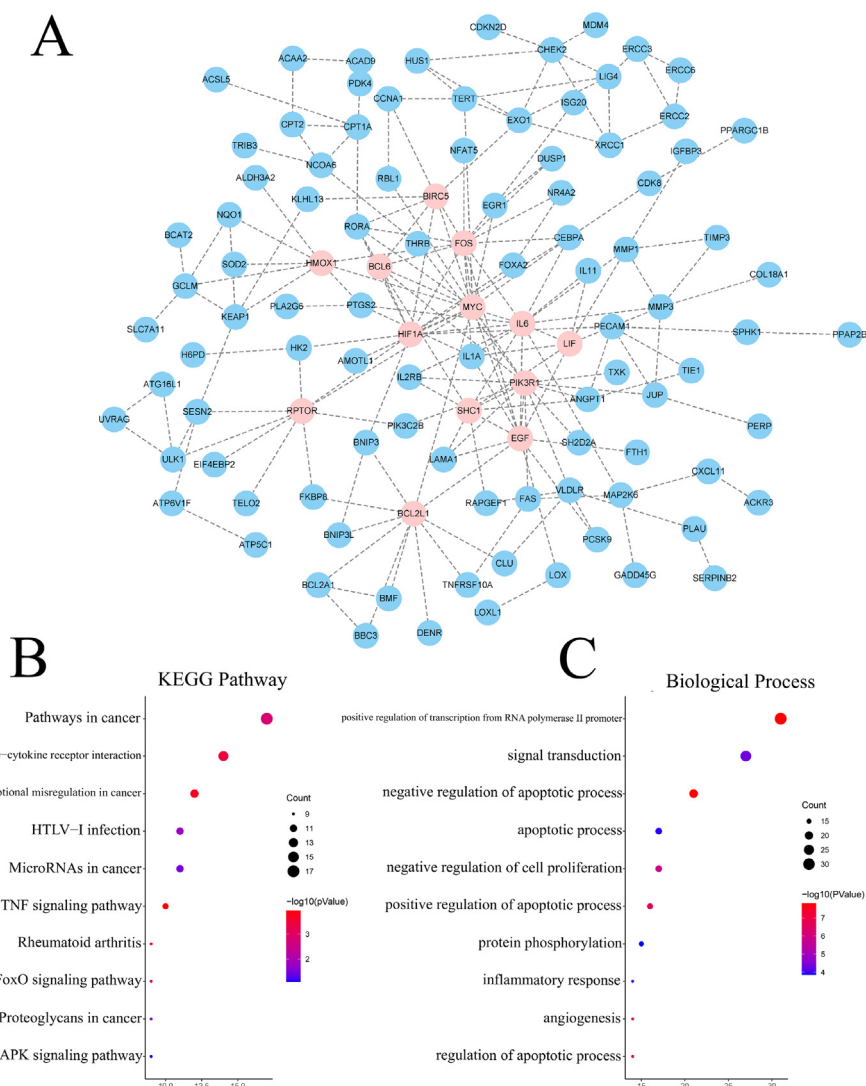


**Fig. 5.** Functional enrichment analysis of overall DEGs and PPI network analysis. (A) The PPI network of 168 DEGs. Light pink nodes represented Hub genes which were calculated by three centrality algorithms. (B) KEGG enrichment analysis on 168 DEGs. (C) GO enrichment analysis on 168 DEGs. (For interpretation of the references to color in this figure legend, the reader is referred to the web version of this article.)

apoptosis and cell cycle via decreasing *MYC* as well as *BIRC5* expression and increasing *EGF* as well as *PIK3R1* expression.

### 3.9. Investigation of potential inhibitors with BRD4 from TSD

It has been reported that *MYC* gene expression is downregulated by knockdown of *BRD4* [30], similarly, TSD could significantly decrease expression of *MYC* gene. Thus, we hypothesized that there exist some inhibitors with *BRD4*. Interestingly, a known *BRD4* inhibitor JQ1 has been reported that can potentially abrogate *MYC* gene expression and cause marked G1 cell-cycle arrest. Then, the model of crystal structure of the first bromodomain of human *BRD4* in complex with the inhibitor JQ1 (PDB ID:3MXF) was selected to launch molecular docking [31]. As a result, Pentagalloylglucose has the lowest binding energy to bromodomain of *BRD4*, forms two major hydrogen-bond interactions with evolutionarily conserved asparagine (Asn140) and a pi-pi stacking interaction with tryptophan (Trp81) (Fig. 7A, S4). Moreover, a comparison of the crystal structure of *BRD4* complexed with cognate ligand JQ1 or with Pentagalloylglucose showed that they are located in the same position, indicating that Pentagalloylglucose may occupy the binding pocket (Fig. 7B). In addition, it has been reported that Pentagal-

loylglucose can arrest the cell cycle at G1 phase and induce apoptosis in Jurkat T cells, whose biological activities are similar with JQ1 [32]. Moreover, we discovered that Pentagalloylglucose (5GG) could significantly decrease the expression of *MYC* gene and reduce c-myc protein expression, indicating it might inhibit the function of *BRD4* (Fig. S5).

## 4. Discussion

It is well known that during the multistep development of human tumors, the hallmarks of cancer comprise six biological capabilities acquired including sustaining proliferation signaling, evading growth suppressors, resisting cell death, enabling replicative immortality, inducing angiogenesis, activating invasion and metastasis [33]. In the present study, TSD exerts an anti-BRCA effects on four biological capabilities by inhibiting proliferation, migration, and inducing G1 cell-cycle arrest as well as apoptosis in BRCA cells. In TCM clinic, TSD has good value in improving the efficacy of chemotherapy by promoting tumor cell apoptosis and blocking angiogenesis, thus it has been widely used in the treatment of BRCA and has clinical value as a whole [34]. Our results from HTS<sup>2</sup> assay suggested that TSD could significantly inhibit

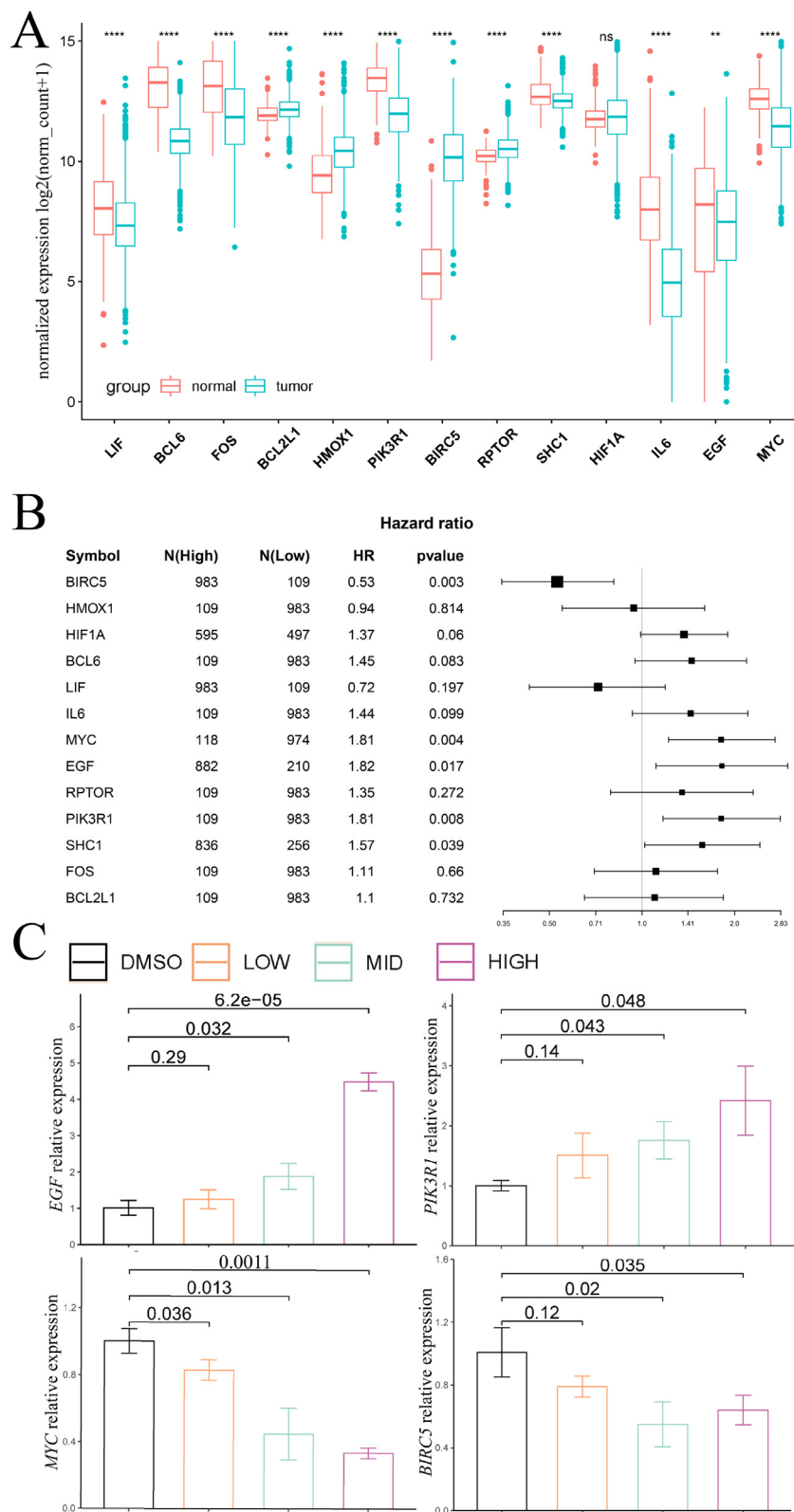


**Fig. 6.** The expression level of hub genes and its related prognosis of BRCA patients, and effect of TSD on selected hub genes. (A) The difference of hub genes expression between BRCA tissue in TCGA database and its normal tissue in TCGA database combined with GTEx database. (B) The forest plot of overall survival analysis on hub genes. (C) Comparative gene expression studies of different-concentration TSD and DMSO.

KRAS pathway and pathway in cancer, and activate apoptosis pathway, p53 pathway and hypoxia pathway. Besides, the “cytokine-cytokine receptor interaction” signaling pathway was also signifi-

cantly enriched, indicating that not only could TSD inhibit oncogenic signaling pathway but it also regulated immune cell signaling. And it has been reported that cytokines show potential

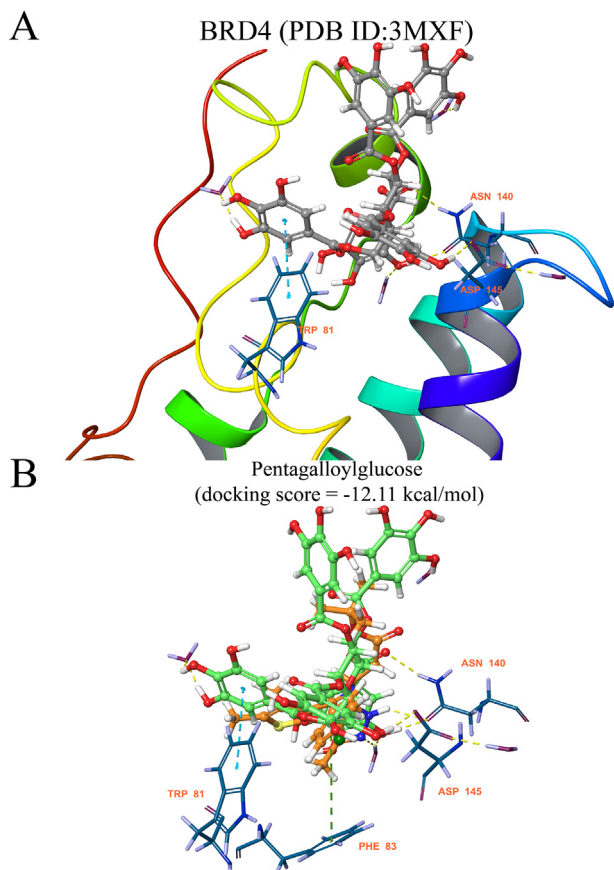


**Fig. 7.** 3D interaction diagrams of BRD4 with potential inhibitors in TSD. (A) Amino acid residues of BRD4 interacting with Pentagalloylglucose. (B) Comparison of cognate ligand JQ1 (orange) with Pentagalloylglucose (green). (For interpretation of the references to color in this figure legend, the reader is referred to the web version of this article.)

in activating host antitumor immunity and inducing tumor regression [35]. Furthermore, six herbs of TSD could be divided into three main categories due to their similarities of gene expression profile. Each group had different functions of regulating biological capabil-

ities associated with cancer cells, which could explain the role of each herb in TSD-treated BRCA.

Underlying mentioned hallmarks of cancer are genome instability. *MYC*, one of the most deregulated oncogenes in human cancers, tightly correlates to cell proliferation, cell cycle and migration [36–37]. *BIRC5*, a member of the inhibitor of apoptosis gene family, encodes negative regulatory proteins named survivin, which lies at the crossroads of a number of cancer cell signaling networks [38]. *EGF*, a growth factor, stimulates cell growth, proliferation and differentiation, and binds to *EGFR* [39]. *PIK3R1*, a tumor-suppressor gene, code for p85 $\alpha$  regulatory subunit of PI3K, which has the function of maintain p110 $\alpha$  catalytic subunit in an inactive conformation [40]. *SHC1* protein serves as intracellular adaptors for several key signaling pathways in BRCA [41]. Taken together, these five genes play an important role in the development and progression of tumor. In addition, they have significant correlation with overall survival in BRCA patients and their transcriptional level are highly significant differences between tumor tissues and adjacent tissues by bioinformatics analysis.

Subsequently, we found that four-fifths of above genes were regulated by TSD, indicating that TSD exerts effects on proliferation, migration, apoptosis and cell cycle in BRCA cells via decreasing *MYC* as well as *BIRC5* expression and increasing *EGF* as well as *PIK3R1* expression. Thus, we hypothesized that there are some active compounds present in TSD to regulate mRNA expression level of four genes. While a therapeutic approach to directly target *MYC*, *BIRC5*, *EGF* or *PIK3R1* has remained elusive, because of the lack of a ligand binding domain. Unfortunately, we had to pay attention to other proteins that can control these genes expression.

Recent research showed that BRD4 is linked to *MYC* dependent transcription and remains bound to transcriptional start sites of genes expressed during the M/G1 transition [42]. Meanwhile, a compelling rationale for targeting BRD4 in cancer has been established. JQ1, the first BRD4 inhibitor, suppresses *MYC* expression and induces G1 cell cycle arrest [30–31]. Consistent with the effect of TSD on MDA-MB-231 cells, we hypothesized that there exist some inhibitors with BRD4 present in TSD. Finally, molecular docking was conducted to identify the potential inhibitors with BRD4. As a result, Pentagalloylglucose may be a potential inhibitor with BRD4. Hence, a series of experiments need carry out to validate that whether Pentagalloylglucose is a BRD4 inhibitor and explore its mechanisms in the future.

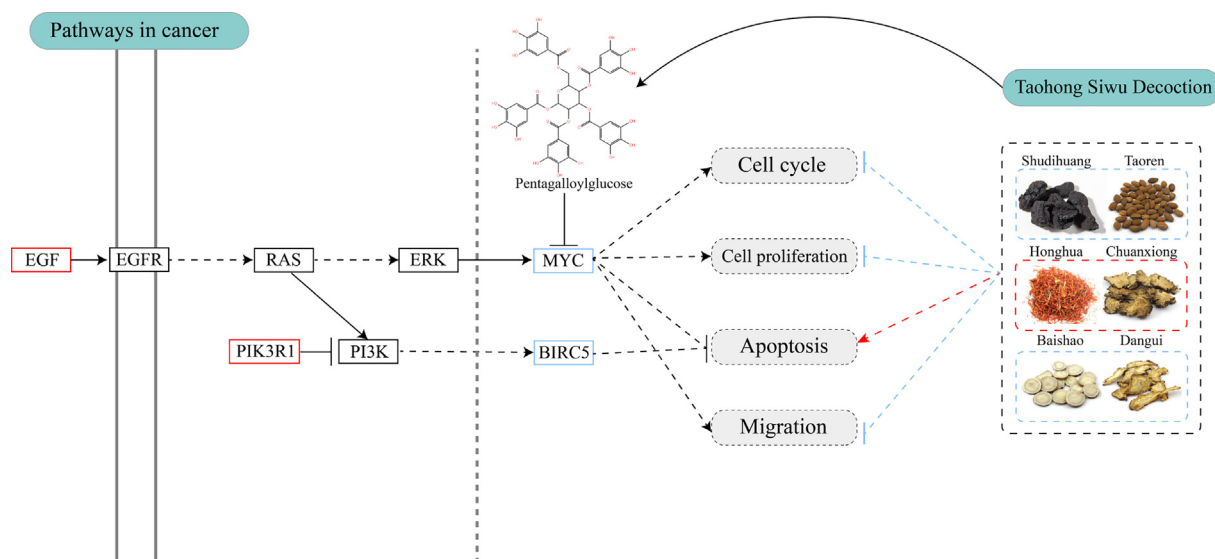


**Fig. 8.** The mechanism of action of TSD in treating BRCA. Arrows represented the activation effect while T-arrows represented the inhibition effect. And the increased expression of genes were marked in red, while the decreased expression of genes were marked in blue. (For interpretation of the references to color in this figure legend, the reader is referred to the web version of this article.)

## 5. Conclusion

In summary, TSD exerts a therapeutic effect on inhibiting proliferation, migration, and inducing G1 phase arrest as well as apoptosis in MDA-MB-231 cells through regulating *MYC*, *BIRC5*, *EGF* and *PIK3R1* expression. And this study reveals the mechanism of action of TSD in treating BRCA (Fig. 8).

## Author contributions

Yu Gui, Yifei Dai, Xilingqi Bao and Dong Wang conceived this study; Yu Gui, Shengrong Li, Lei Xiang, Yuqin Tang, Xue Tan, and Tianli Pei performed the experiments; Yu Gui, Yifei Dai and Yumei Wang collected the data; Yu Gui wrote the manuscript; Yu Gui, Yifei Dai, Yumei Wang, Yuqin Tang, and Dong Wang edited the manuscript; and all authors read and gave final approval to submit the manuscript.

## Declaration of competing interest

The authors declare that they have no known competing financial interests or personal relationships that could have appeared to influence the work reported in this paper.

## Acknowledgments

This work was supported by Key Projects of Science and Technology Plan of Inner Mongolia Autonomous Region (201802115), the National Natural Science Foundation of China (Grant No. 82172723, 81673460), Science and Technology Department of Sichuan Province (Grant No. 2021ZYD0079), and the Sichuan Youth Science and Technology Innovation Research Team of Experimental Formology (2020JDTD0022).

## Appendix A. Supplementary data

Supplementary data to this article can be found online at <https://doi.org/10.1016/j.csbj.2022.06.044>.

## References

- [1] Azamjah N, Soltan-Zadeh Y, Zayeri F. Global Trend of Breast Cancer Mortality Rate: A 25-Year Study. *Asian Pac J Cancer Prev* 2019;20(7):2015–20. <https://doi.org/10.31557/APJCP.2019.20.7.2015>.
- [2] Wu Z, Wu J, Zhao Q, et al. Emerging roles of aerobic glycolysis in breast cancer. *Clin Transl Oncol* 2020;22(5):631–46. <https://doi.org/10.1007/s12094-019-02187-8>.
- [3] Yeo SK, Guan JL. Breast Cancer: Multiple Subtypes within a Tumor? *Trends Cancer* 2017;3(11):753–60. <https://doi.org/10.1016/j.trecan.2017.09.001>.
- [4] Qi F, Zhao L, Zhou A, et al. The advantages of using traditional Chinese medicine as an adjunctive therapy in the whole course of cancer treatment instead of only terminal stage of cancer. *Biosci Trends* 2015;9(1):16–34. <https://doi.org/10.5582/bst.2015.01019>.
- [5] Duan X, Pan L, Bao Q, et al. UPLC-Q-TOF-MS Study of the Mechanism of THSWD for Breast Cancer Treatment. *Front Pharmacol* 2020;10:1625. <https://doi.org/10.3389/fphar.2019.01625>.
- [6] Yang H, Tong C, Chu A, et al. Effect of Tao Hong Siwu Decoction on Angiogenesis in Patients with Breast cancer (in Chinese). *J Guangzhou Univ Tradit Chin Med* 2012;29(06):623–6. <https://doi.org/10.13359/j.cnki.gzxbtcm.2012.06.028>.
- [7] Fu S, He Y, Wang N, et al. Effects of Taohong Siwu Decoction on Protein Expression of Bcl-2, Bax, and Ki-67 in Invasive Breast Cancer (in Chinese). *Acta Chinese Medicine and Pharmacology* 2018;46(04):89–92. <https://doi.org/10.19664/j.cnki.1002-2392.180124>.
- [8] Huang L, Yi X, Yu X, et al. High-Throughput Strategies for the Discovery of Anticancer Drugs by Targeting Transcriptional Reprogramming. *Front Oncol* 2021;11:1. <https://doi.org/10.3389/fonc.2021.762023>.
- [9] Shao W, Li S, Li L, et al. Chemical genomics reveals inhibition of breast cancer lung metastasis by Ponatinib via c-Jun. *Protein Cell* 2019;10(3):161–77. <https://doi.org/10.1007/s13238-018-0533-8>.
- [10] Dai Y, Qiang W, Gui Y, et al. A large-scale transcriptional study reveals inhibition of COVID-19 related cytokine storm by traditional Chinese

- medicines. *Sci Bull (Beijing)* 2021;66(9):884–8. <https://doi.org/10.1016/j.scib.2021.01.005>.
- [11] Dai Y, Qiang W, Yu X, et al. Guizhi Fuling Decoction inhibiting the PI3K and MAPK pathways in breast cancer cells revealed by HTS2 technology and systems pharmacology. *Comput Struct Biotechnol J* 2020;18:1121–36. <https://doi.org/10.1016/j.csbj.2020.05.004>.
- [12] Li H, Zhou H, Wang D, et al. Versatile pathway-centric approach based on high-throughput sequencing to anticancer drug discovery. *Proc Natl Acad Sci U S A* 2012;109(12):4609–14. <https://doi.org/10.1073/pnas.1200305109>.
- [13] Bayat A. Science, medicine, and the future: Bioinformatics. *BMJ* 2002;324(7344):1018–22. <https://doi.org/10.1136/bmi.324.7344.1018>.
- [14] Zhang W, Huai Y, Miao Z, et al. Systems Pharmacology for Investigation of the Mechanisms of Action of Traditional Chinese Medicine in Drug Discovery. *Front Pharmacol* 2019;10:743. <https://doi.org/10.3389/fphar.2019.00743>.
- [15] Ru J, Li P, Wang J, et al. TCMSPP: a database of systems pharmacology for drug discovery from herbal medicines. *J Cheminform* 2014;6:13. <https://doi.org/10.1186/1758-2946-6-13>.
- [16] Xue R, Fang Z, Zhang M, et al. TCMIID: Traditional Chinese Medicine integrative database for herb molecular mechanism analysis. *Nucleic Acids Res.* 2013;41(Database issue):D1089–D1095. doi:10.1093/nar/gks1100.
- [17] Daina A, Michielin O, Zoete V. SwissTargetPrediction: updated data and new features for efficient prediction of protein targets of small molecules. *Nucleic Acids Res* 2019;47(W1):W357–64. <https://doi.org/10.1093/nar/gkz382>.
- [18] Amberger JS, Bocchini CA, Schiettecatte F, et al. OMIM.org: Online Mendelian Inheritance in Man (OMIM®), an online catalog of human genes and genetic disorders. *Nucleic Acids Res.* 2015;43(Database issue):D789–D798. doi:10.1093/nar/gku1205.
- [19] Wishart DS, Feunang YD, Guo AC, et al. DrugBank 5.0: a major update to the DrugBank database for 2018. *Nucleic Acids Res* 2018;46(D1):D1074–82. <https://doi.org/10.1093/nar/gkx1037>.
- [20] Wang Y, Zhang S, Li F, et al. Therapeutic target database 2020: enriched resource for facilitating research and early development of targeted therapeutics. *Nucleic Acids Res* 2020;48(D1):D1031–41. <https://doi.org/10.1093/nar/gkz981>.
- [21] Love MI, Huber W, Anders S. Moderated estimation of fold change and dispersion for RNA-seq data with DESeq2. *Genome Biol* 2014;15(12):550. <https://doi.org/10.1186/s13059-014-0550-8>.
- [22] Wickham H: ggplot2: Elegant Graphics for Data Analysis. Springer-Verlag New York, 2016; ISBN 978-3-319-24277-4. doi:10.1007/978-3-319-24277-4.
- [23] Subramanian A, Tamayo P, Mootha VK, et al. Gene set enrichment analysis: a knowledge-based approach for interpreting genome-wide expression profiles. *Proc Natl Acad Sci U S A* 2005;102(43):15545–50. <https://doi.org/10.1073/pnas.0506580102>.
- [24] von Mering C, Huynen M, Jaeggi D, et al. STRING: a database of predicted functional associations between proteins. *Nucleic Acids Res* 2003;31(1):258–61. <https://doi.org/10.1093/nar/gke034>.
- [25] Shannon P, Markiel A, Ozier O, et al. Cytoscape: a software environment for integrated models of biomolecular interaction networks. *Genome Res* 2003;13(11):2498–504. <https://doi.org/10.1101/gr.1239303>.
- [26] Huang DW, Sherman BT, Tan Q, et al. DAVID Bioinformatics Resources: expanded annotation database and novel algorithms to better extract biology from large gene lists. *Nucleic Acids Res.* 2007;35(Web Server issue):W169–W175. doi:10.1093/nar/gkm415.
- [27] Cancer Genome Atlas Research Network, Weinstein JN, Collisson EA, et al. The Cancer Genome Atlas Pan-Cancer analysis project. *Nat Genet.* 2013;45(10):1113–1120. doi:10.1038/ng.2764.
- [28] . *Nat Genet* 2013;45(6):580–5. <https://doi.org/10.1038/ng.2653>.
- [29] Berman HM, Westbrook J, Feng Z, et al. The Protein Data Bank. *Nucleic Acids Res* 2000;28(1):235–42. <https://doi.org/10.1093/nar/28.1.235>.
- [30] Shao Q, Kannan A, Lin Z, et al. BET protein inhibitor JQ1 attenuates Myc-amplified MCC tumor growth in vivo. *Cancer Res* 2014;74(23):7090–102. <https://doi.org/10.1158/0008-5472.CAN-14-0305>.
- [31] Filippakopoulos P, Qi J, Picaud S, et al. Selective inhibition of BET bromodomains. *Nature* 2010;468(7327):1067–73. <https://doi.org/10.1038/nature09504>.
- [32] Chen WJ, Lin JK. Induction of G1 arrest and apoptosis in human jurkat T cells by pentagalloylglucose through inhibiting proteasome activity and elevating p27Kip1, p21Cip1/WAF1, and Bax proteins. *J Biol Chem* 2004;279(14):13496–505. <https://doi.org/10.1074/jbc.M212390200>.
- [33] Hanahan D, Weinberg RA. Hallmarks of cancer: the next generation. *Cell* 2011;144(5):646–74. <https://doi.org/10.1016/j.cell.2011.02.013>.
- [34] Jiang H, Li M, Du K, et al. Traditional Chinese Medicine for adjuvant treatment of breast cancer: Taohong Siwu Decoction. *Chin Med* 2021;16(1):129.
- [35] Zhang J, Zhao X. Administration of fusion cytokines induces tumor regression and systemic antitumor immunity. *MedComm (2020)*. 2021;2(2):256–268.
- [36] Bretones G, Delgado MD, León J. Myc and cell cycle control. *Biochim Biophys Acta* 2015;1849(5):506–16. <https://doi.org/10.1016/j.bbagr.2014.03.013>.
- [37] Wang T, Cai B, Ding M, et al. c-Myc Overexpression Promotes Oral Cancer Cell Proliferation and Migration by Enhancing Glutaminase and Glutamine Synthetase Activity. *Am J Med Sci* 2019;358(3):235–42. <https://doi.org/10.1016/j.amjms.2019.05.014>.
- [38] Li F, Aljahlali I, Ling X. Cancer therapeutics using survivin BIRC5 as a target: what can we do after over two decades of study? *J Exp Clin Cancer Res* 2019;38(1):368. <https://doi.org/10.1186/s13046-019-1362-1>.
- [39] Wilson KJ, Gilmore JL, Foley J, et al. Functional selectivity of EGF family peptide growth factors: implications for cancer. *Pharmacol Ther* 2009;122(1):1–8. <https://doi.org/10.1016/j.pharmthera.2008.11.008>.

- [40] Vallejo-Díaz J, Chagoyen M, Olazabal-Morán M, et al. The Opposing Roles of PIK3R1/p85 $\alpha$  and PIK3R2/p85 $\beta$  in Cancer. *Trends Cancer* 2019;5(4):233–44. <https://doi.org/10.1016/j.trecan.2019.02.009>.
- [41] Wright KD, Miller BS, El-Meanawy S, et al. The p52 isoform of SHC1 is a key driver of breast cancer initiation. *Breast Cancer Res.* 2019;21(1):74. Published 2019 Jun 15. doi:10.1186/s13058-019-1155-7.
- [42] Dey A, Nishiyama A, Karpova T, et al. Brd4 marks select genes on mitotic chromatin and directs postmitotic transcription. *Mol Biol Cell* 2009;20(23):4899–909. <https://doi.org/10.1091/mbc.e09-05-0380>.